Periodico di Mineralogia (2015), 84, 3A (Special Issue), 407-418 DOI: 10.2451/2015PM0021

PERIODICO di MINERALOGIA
established in 1930

An International Journal of
MINERALOGY, CRYSTALLOGRAPHY, GEOCHEMISTRY,
ORE DEPOSITS, PETROLOGY, VOLCANOLOGY
and applied topics on Environment, Archaeometry and Cultural Heritage

Hyperspectral imaging-based approach for the in-situ characterization of ancient Roman wall paintings

Giuseppe Capobianco[1,*], Fernanda Prestileo[2], Silvia Serranti[1] and Giuseppe Bonifazi[1]

[1] Dipartimento Ingegneria Chimica Materiali Ambiente (DICMA)
Sapienza Università di Roma, Via Eudossiana, 18, I-00184 Rome, Italy
[2] Istituto per la conservazione e valorizzazione dei beni culturali
(ICVBC), Consiglio Nazionale delle Ricerche
Via Salaria Km 29,300, C.P. 10, 00015 Monterotondo St., Rome, Italy
[*] Corresponding author: *giuseppe.capobianco@uniroma1.it*

Abstract

A diagnostic study was recently carried out on fragments of wall paintings belonging to the decorations of an old Roman residential villa of the Ager Gabinus, in the locality Pratolungo (Rome, Italy). The study was organized in two stages. A first stage, in which small fragments of these painted specimens were embedded in resin to obtain polished and thin cross-sections to study by optical microscopy and a second phase, in which the specimens were analyzed by Raman Spectrometry and HyperSpectral Imaging (HSI). The results obtained by classical methods (i.e. optical microscopy), were compared with those resulting from non-destructive investigation such as, Raman spectroscopy and HSI based techniques. The attention was particularly addressed to the use of HSI in the SWIR range (1000-2500 nm), being this techniques potentially used directly in situ without any physical sampling/removal of the specimen of interest. The collected hyperspectral data (i.e. images) were processed applying chemometric methods. The use of HSI as a diagnostic tool in the field of cultural heritage is of great interest and it presents high potentialities, being this analysis intrinsically non-destructive, non-invasive and in principle applicable in any site. Furthermore, the possibility to couple hyperspectral data with chemometric techniques allows getting not only qualitative but also quantitative information on the nature and the physical-chemical attributes and characteristics of the investigated materials. Following this strategy, it is thus possible to obtain information comparable with those commonly acquired by optical microscopy, allowing also the identification of pigments and the constituent materials directly in situ.

Key words: wall paintings; hyperspectral imaging; Raman spectroscopy; chemometric methods; optical microscopy.

Introduction

HyperSpectral Imaging (HSI), in these last years, has been more and more utilized, in the field of cultural heritage, to perform materials characterization (Cucci et al., 2013; Capobianco et al., 2014a). HSI is of particular interest to perform studies finalized to evaluate, quantify and spatially define alteration processes affecting painting materials in old wall decorations. These analyses are usually quite challenging to carry out mainly for the complexity of the phenomena affecting the original utilized painting products and the variety of alteration mechanisms, as well as interactions among them and the environmental conditions. Old paintings usually contain pigments, mainly mineral phases, and specific binding media such as calcium carbonate, protein binders, etc.. Painting materials are sensitive to the influence of atmospheric pollution, humidity, temperature and varying environmental conditions associated with climate change. To successfully develop procedures and studies able to properly quantify these effects on old wall paintings is thus fundamental to utilize advanced analytical techniques. Raman and Infrared Spectroscopies, as well as classical Optical Microscopy based devices, can be particularly useful to reach these goals, providing a large and detailed information about chemical composition and structural features of inorganic and organic compounds. Furthermore, due to the large quantities and the complexity of the data to handle, sophisticated statistical and mathematical methods have to be applied, often requiring the development and set up of specific algorithms, usually based on Chemometric Methods.

HSI is based on the collection of images (2D data), of a given scene, at different wavelengths in a wide spectral region, typically in the range VIS–NIR (400-1000 nm) and SWIR (1000-2500 nm). The acquired data set, constituted by spectra referred to each cell image (i.e. pixel), generates the image itself. With reference to wall paintings, reflectance spectra can be thus utilized to perform a non-invasive identification of "pictorial materials" (i.e. pigments, dyes, preparation layer, products of alteration, etc.) constituting them. The collected HSI data set is usually processed utilizing multivariate analysis (Principal Component Analysis, Multivariate Curve Resolution, etc.) in order to obtain information regarding presence and distribution of the various elements on the painted surface. The main aim of this study was thus to perform a comparison of the proposed innovative HSI based approach with other consolidate techniques of analysis for the characterization of materials, such as optical microscopy, in reflected and transmitted light, and Raman spectroscopy. Furthermore, the potential benefits of the combined utilization of HSI technique and chemometric analysis in order to perform investigations directly in situ, without any physical sampling/removal of the specimen of interest, are highlighted.

Materials and methods

Sample preparation

Seven fragments of painted mortars, characterized by different colouring and alteration of the surfaces, were collected and investigated. Samples were consecutively numbered from 1 to 7. Their characteristics are synthetically reported in Table 1 and Figure 1. Starting from these samples, both polished and thin cross-sections have been prepared. Polished sections have been utilized to perform Raman spectroscopy, optical microscopy and HSI based analyses. Thin sections have been utilized to perform "only" optical microscopy based analyses.

Equipments

A SciAps Raman Advantage 785™ spectrometer, with a spectral range 200-2500

cm^{-1} and resolution of 3-5 cm^{-1} was utilized to perform Raman spectroscopy analyses. These analyses have been preliminary carried out in order to obtain qualitative information on the compositions of the fragments, allowing to better localize the area for the next micro-sampling, finalized to understand both sample surface status, as well as painting layers composition and characteristics. Optical microscopy analyses have been carried out utilizing a Leica DM EP microscopy, 3 levels of magnification: 50x, 100x, 200x have been utilized. Both polished and this cross-sections of each selected samples were investigated in order i) to characterize the sequence of the surface layers present on the mortar, of its components, ii) to identify any possible artificial treatments and, finally, iii) to determine the pigments. Hyperspectral analyses have been performed by a Specim SISUChema XL™, embedding an ImSpector™ N25E (Specim Ltd, Finland) acting in the range from 1000 to 2500 nm, with a spectral sampling/ pixel of 6.3 nm, coupled with a MCT camera (320 x 240 pixels). Pixel resolution is 14 bits. HSI was applied in order to identify and map the pigments present on each plaster fragment surface, determining, at the same time, their state of conservation.

Raman and hyperspectral data processing

Raman and hyperspectral collected data have been analysed adopting Chemometric Methods

Table 1. Main characteristics of the seven plaster samples.

Sample identification code	Sample estimated surface area (cm^2)	Description
GV01	40	The sample surface presents a yellow colour partially covered by a deposit (Figure 1a)
GV02	32	The sample is characterized by a smooth white layer on the surface, partly covered by a deposit (Figure 1b)
GV03	24	The sample is characterized by a yellow layer on the surface. Traces of decoration, partly covered by a surface deposit, (Figure 1c) can also be identified
GV04	6	The sample is characterized by a reddish surface layer, partly covered by a surface deposit (Figure 1d)
GV05	30	Traces of red decoration on the surface and a smooth white layer on the remaining sample (Figure 1e) characterize it
GV06	8	A yellow surface layer, partly covered by a surface deposit, (Figure 1f) is the main element characterizing this sample
GV07	12	The sample is characterized by a yellow surface layer partly covered by a surface deposit (Figure 1g)

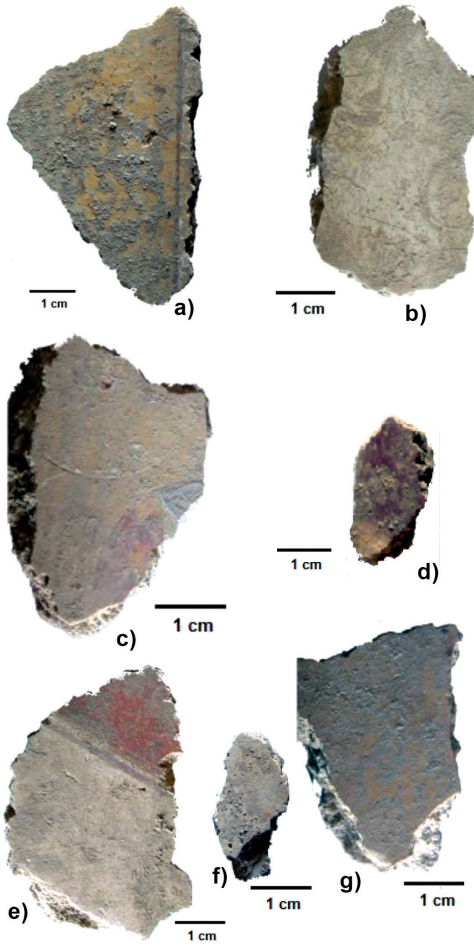

Figure 1. Investigated samples.

(Geladi et al., 2007). To reach this goal, the Toolbox software (Version 7.8 Eigenvector Research, Inc.), running inside Matlab (Version 7.11.1, The Mathworks, Inc.), has been used. Data have been preliminary analysed by Principal Component Analysis (PCA), then a Partial Least Square Discriminant Analysis (PLS-DA) was applied.

PCA is a useful method capable of providing an overview of complex multivariate data (Bro and Smilde, 2014). PCA can be used for revealing relations between variables and relations between samples (e.g. clustering), detecting outliers, finding and quantifying patterns, generating new hypotheses as well as many other things. It was used to decompose the "processed" spectral data into several Principal Components (PCs) (linear combinations of the original spectral data), embedding the spectral variations of each collected spectral data set. According to this approach, a reduced set of factors is produced. Such a set can be used for discrimination, since it provides an accurate description of the entire dataset. The first few PCs are generally used to analyses the common features among samples and their grouping: in fact, samples characterized by similar spectral signatures tend to aggregate in the score plot of the first two or three components. Spectra could be thus characterized either by the reflectance at each wavelength in the wavelength space, or by their score on each PC in the PC space. Samples characterized by similar spectra, which belong to the same class of products, are grouped in the same region of the score plot related to the first two or three PCs, whereas samples characterized by different spectral features will be clustered in other parts of this space.

PLS-DA is a linear classification method combining the properties of partial least squares regression with the discrimination power of a classification technique (Ballabio and Consonni, 2013). PLS-DA is based on the PLS regression algorithm (PLS1 when dealing with one dependent Y variable and PLS2 in the presence of several dependent Y variables), which searches for latent variables with a maximum covariance with the Y-variables. The main advantage of PLS-DA is that the relevant sources of data variability are modelled by the so-called Latent Variables (LVs), which are a linear combinations of the original variables, and, consequently, it allows graphical

visualization and understanding of the different data patterns and relations by LV scores and loadings. Loadings are the coefficients of variables in the linear combinations which determine the LVs and therefore they can be interpreted as the influence of each variable on each LV, while scores represent the coordinates of samples in the LV projection hyperspace.

Results

Raman spectroscopy

Fifty five measurements were performed on different regions of each fragment. As previously outlined, this approach was followed in order to identify the most significant areas to utilise for micro-sampling.

Raman spectroscopy evidenced the presence of three families of spectra (Figure 2). They show peaks around 1086, 339 and 276 cm^{-1}, which can be attributed to the presence of calcium carbonate. Peaks at 338 and 246 cm^{-1} are due to vermilion. Peaks at 403 cm^{-1}, 285 and 219 cm^{-1} are generated by the presence of iron oxides, compatible with the presence to ochre pigment; finally the peak at 1008 cm^{-1} is due to the presence of gypsum (Bevilacqua et al., 2010).

Smoothing, Normalize and Mean Centering pre-processing were applied before PCA modelling. The variance captured in six components is 89.76%. The score plot shows three separate groups (Figure 3a). Group A is associated with the presence of ochre and calcite, group B with calcite and group C with calcite and vermilion. In the second graph (Figure 3b) the representative points of the investigated region, referred to a specific sample, are outlined. The analysis of this plot shows as iron oxides are present also in sample GV04, while the presence of vermilion is also detected in GV03 GV05 samples. The presence of calcium carbonate in all samples (Group B) is in accordance with the usual composition of the mortars used for Roman wall paintings.

Optical microscopy

The analyses carried out by optical microscopy allowed for determining the characteristics of the different layers (i.e. different materials/ products). In the sample GV01 (Figure 4a),

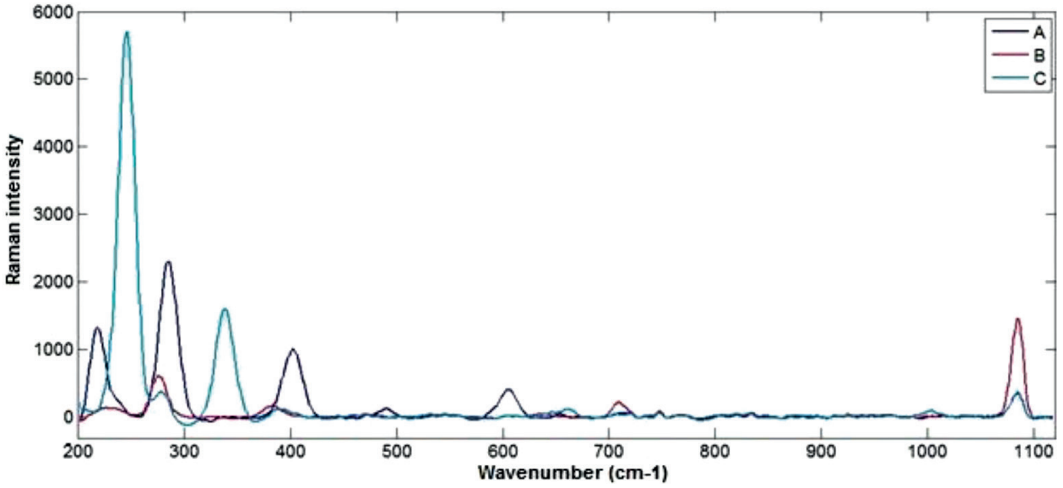

Figure 2. Mean spectra of groups of different composition (A, B and C) as resulting from Raman spectroscopy applied to different regions of plaster fragments.

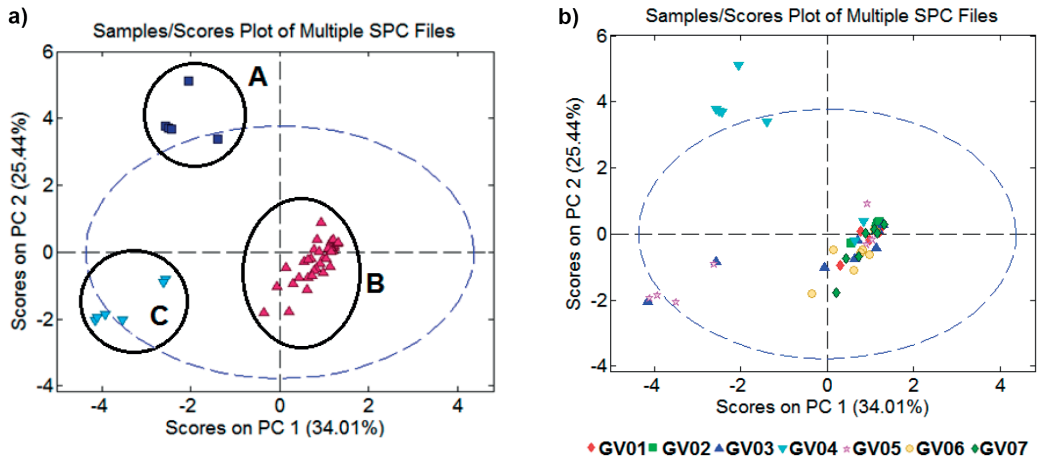

Figure 3. PC1-PC2 score plot of the collected Raman data, referred to the three groups identified by the principal component analysis (a) and referred to the distribution of the measurements carried out on each sample, from GV1 to GV7 (b). Group A can be considered representative of sample area where the presence of ochre and calcite is detected, group B with only the presence of calcite, and group C with calcite and vermilion.

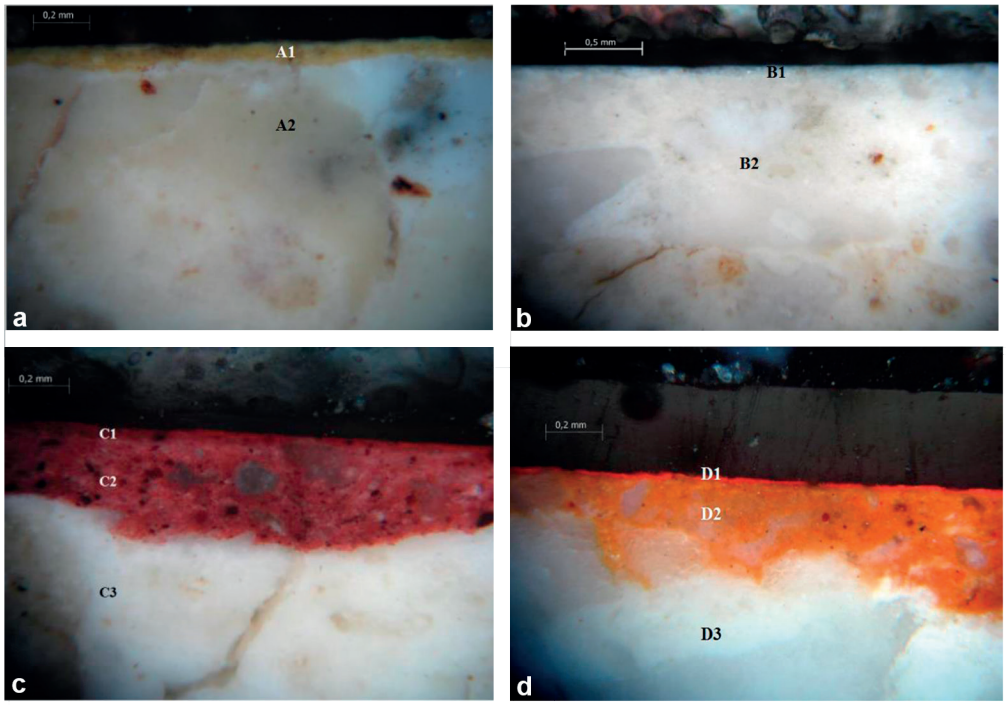

Figure 4. Microphotographs of samples polished cross-sections: (a) sample GV01; (b) sample GV02; (c) sample GV04; and (d) sample GV05. (a), (c) and (d) magnification 100x; (b) magnification 50x.

starting from the surface, a yellow opaque almost continuous layer, characterized by a thickness of about 0.8 µm, was found (Figure 4a - A1). Such a layer is composed of a light yellow binder and abundant whitish-translucent sharp edges elements (Figure 4a - A1). Analyses showed as it was applied without break in continuity. Its surface is quite regular and well-binded with the underlying layer. The white preparation layer (i.e. mortar) is constituted by a whitish-translucent sharp edges elements medium-fine aggregates (Figure 4a - A2).

Sample GV02 (Figure 4b) is characterized by a white finishing layer, with a continuous thickness of about 0.6 µm, it results constituted by a whitish binder and a fine sharp edges whitish-translucent aggregate (Figure 4b - B1). The red covering layer, in sample GV04 (Figure 4c), is characterized by an almost continuous thickness of about 40 µm (Figure 4c - C1) and under the red opaque layer, an another red layer with a thickness from 150 to 350 µm (Figure 4c - C2) can be detected.

Sample GV05 is characterized by a continuous red color of ana average thickness of about 25 µm (Figure 4d - D1) and under the red layer there is an orange layer with a thickness from 200 to 400 µm (Figure 4d - D2).

Sample GV06 shows the same characteristics already described for sample GV02.

A flattening is applied on the surfaces of all samples. The whitish mortar preparation is the same for all the samples and it is composed by a whitish binder and a whitish-translucent individuals characterized by sharp edges ranging between silty to medium-fine arenaceous aggregates. Its thickness is about 5 mm. This cover results composed of a light-colored binder and abundant gray and opaque elements with sharp edges, it is applied in two layers: the first composed of aggregates of an average size of about 38 µm and the second, about 1.2 µm thick, and it is smoothed utilizing very fine aggregates. The surface results quite regular and well-tied with the underlying layer.

The whitish mortar preparation, with a continuous average thickness of about 6 mm, is constituted by a whitish binder and whitish-

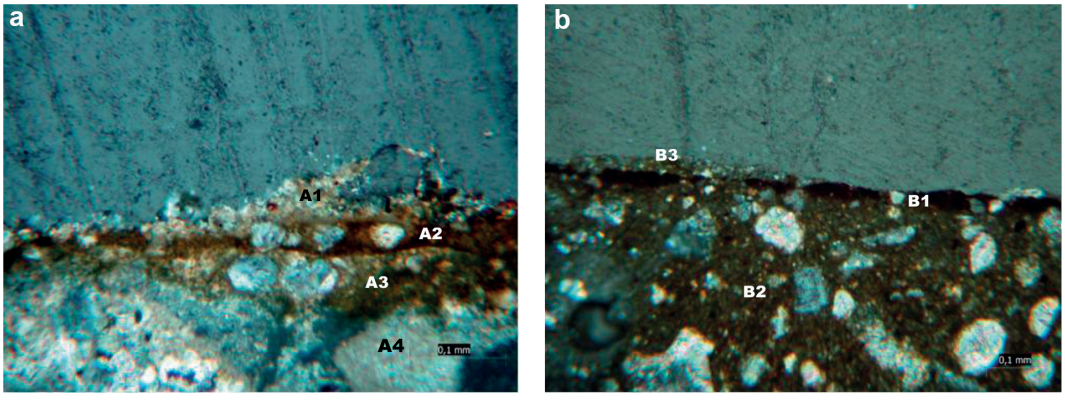

Figure 5. Microphotographs of sample thin sections: (a) sample GV01 (magnification 500x) and (b) sample GV05 (magnification 100x). Sample GV01 - A1 = lime altered by sulphation, A2 = binder, lime and yellowish/ochre pigment A3 = pigmented opaque amorphous binder and A4 = lime-binder and fine and sparse sharp edges blackish and yellowish pigments. Sample GV05 - B1 = pigmented opaque amorphous binder and fine sharp edges carbonate particles and B2 = lime-binder and fine and sparse sharp edges blackish and yellow pigments.

translucent aggregates characterized by sharp edges and, as for samples GV02 (Figure 4b - B2), GV04 (Figure 4c - C3), GV05 (Figure 4d - D3), with a size class distribution ranging between silty to medium-fine sandstone aggregates. The surface is quite regular and well tied with the underlying layer.

The analyses of the thin sections of the samples characterized by a yellow surface showed the presence of a yellowish/ochre homogeneous layer surface (Figure 5a), with a thickness of about 40 μm, composed of a pigmented opaque amorphous binder and from abundant and fine sharp edges carbonate individuals (Figure 5a - A2). Then, a layer with an almost continuous thickness of about 40 μm (Figure 5a - A3), composed of a binder and lime with abundant yellowish/ochre pigment, is identified ((Figure 5a - A3). On the surface of the thin section, an irregular lime layer, altered by sulphation, can be observed (Figure 5a - A1). Underneath this altered surface, a layer, of about 300 μm thick, composed of a lime-binder and fine and sparse sharp edges blackish individuals can be identified (Figure 5a - A4). In the thin sections of the samples characterized by red colour, the presence of a homogeneous dark-red layer (Figure 5b - B1) can be easily detected. Layer shows a thickness of about 30 μm, consisting of a pigmented opaque amorphous binder and fine sharp edges carbonate particles. Then a continuous layer, with a thickness of about 400 μm, and consisting of a lime-binder and abundant ochre pigments, is also present (Figure 5b - B2).The surfaces of all examined samples are characterized by the presence of irregular layers probably due to sulphation (Figure 5b - B3).

Hyperspectral imaging

The hyperspectral analyses, carried out in the SWIR range, confirmed the presence of calcium carbonate in all samples, as outlined by the presence of absorptions between 2100 and 2400 nm (Gaffey, 1986). The main differences between the various groups are concentrated in the wavelength field ranging between 1000 and 1200 nm.

The hypothesized material on the surface of the analyzed samples is mainly composed of gypsum, with a fork absorptions identified in the interval 1400-1600 nm, and calcite, with absorptions in 2100-2400 nm range (Bevilacqua et al., 2010). The average values of the spectra collected in different regions of the samples according to their surface characteristics are reported in Figure 6. Based on the previously discussed Raman analysis, performed to identify physical-chemical attributes of specific mortar surfaces (i.e. painting layers), several Region of Interest (ROI) were selected on all samples, and the corresponding spectra acquired, in order to create an HSI-based model to be used for recognition and classification of sample surface attributes.

Standard Normal Variate (SNV) and Mean Centering pre-processing were applied before PCA modelling. The variance captured in six components is 97.65%. The score plot of PC1 and PC2 (Figure 7) show 6 distinct groups that can be attributed to the presence of the various pigments mixed with calcium carbonate, also in the class called “deposit” the presence of two separate clouds of pixels can be attributed to the different composition of the surface deposit detected in the samples.

The same pre-processing approach was then applied to build PLS-DA model. A Cross Validation adopting the “venetian blind method”, with 10 splits and 5 samples for split, was applied. Percent variance captured by regression model with 8 latent variable is 99.84%. The detail of PLA-DA are reported in Table 2. Samples classification adopting the developed PLS-DA model allowed to map the “deposit” (i.e. alteration material present on the surface of each sample) and to identify pigments underneath the surface deposit that cannot be removed (Capobianco et al., 2014b).

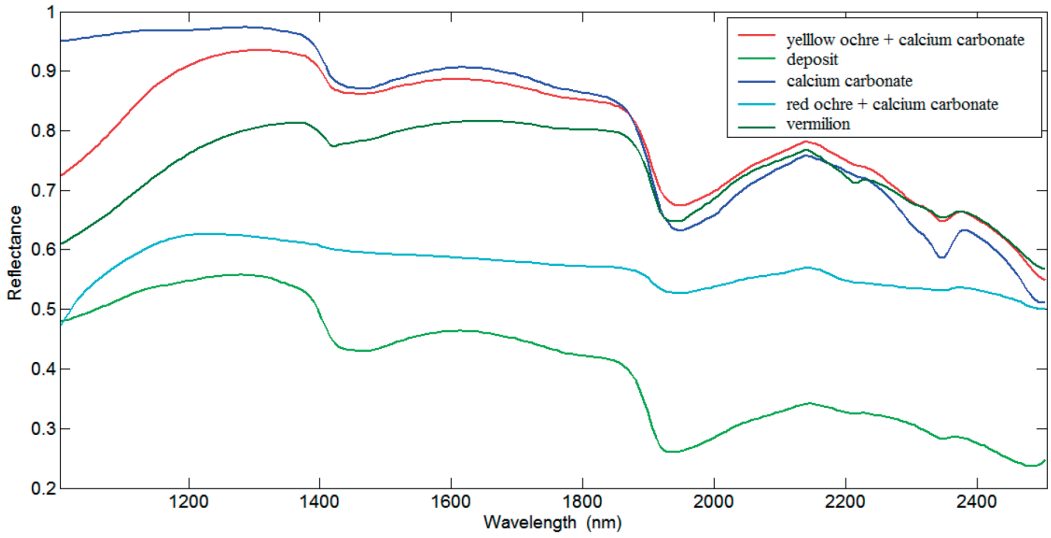

Figure 6. Mean spectra of pixels belonging to different selected Region of Interest (ROI) on samples GV01, GV02 and GV05.

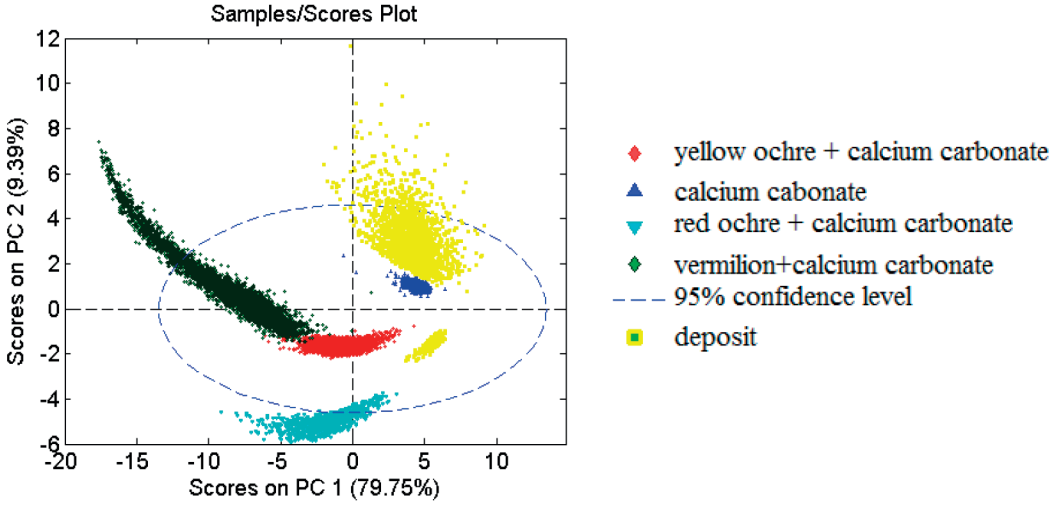

Figure 7. PC1-PC2 score of the collected hyperspectral data.

Table 2. Detail of PLS-DA model.

Modeled Class	Yellow ochre	Deposit	Calcium carbonate	Red ochre + Calcium carbonate	Cinnabar + Calcium carbonate
Sensitivity (in calibration)	0.975	0.977	1.000	0.995	1.000
Specificity (in calibration)	0.975	0.992	1.000	0.991	0.993
Sensitivity (in cross validation)	0.975	0.977	1.000	0.995	1.000
Specificity (in cross validation)	0.974	0.992	1.000	0.991	0.993
Classification Error (in calibration)	0.0251067	0.0155063	0.000207194	0.00719728	0.00354869
Classification Error (in cross validation)	0.0250596	0.0155333	0.000227913	0.0073179	0.00368591

In particular, in the sample GV01 traces of vermilion mixed with calcite can be revealed in the decorative line (Figure 8a).

PLS-DA classification applied to GV01 and GV07 samples, showed as they are similar (Figures 8a and 8g). The white finishing layer, visible in all examined samples, is made of calcium white. Only in sample GV04 (Figure 8d) red ochre without vermilion is present. Vermilion was detected on sample GV01, GV03 (Figure 8c), GV05 (Figure 8e). Yellow ochre mixed with calcite is also detected on sample GV01, GV03, GV06 (Figure 8f) and GV07.

Conclusions

In the present paper, a full characterization of the materials in ancient Roman painting samples, was performed. Such a goal was reached comparing the results achievable by well-established investigation techniques (i.e. optical reflected/ transmitted light microscopy and Raman spectroscopy) applied on thin and polished cross-sections with innovative non-destructive methods HyperSpectral Imaging (HIS) based. The combination of information derived from the three analytical approaches allowed to fully characterize the

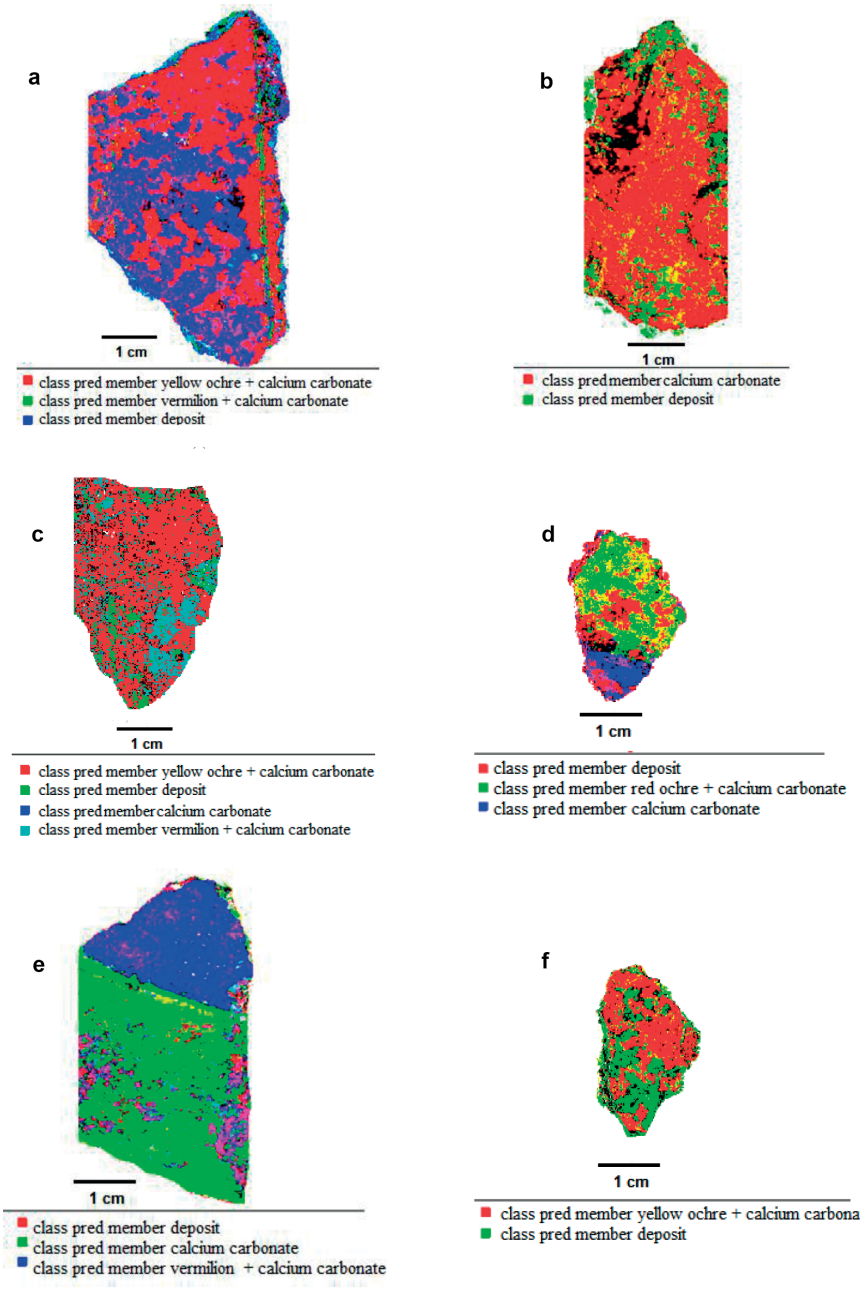

Figure 8. Result of Partial Least Square Discriminant Analysis (PLS-DA) classification for all the analysed samples. (a) sample GV01, (b) sample GV02, (c) sample GV03, (d) sample GV04, (e) sample GV05, (f) sample GV06 and (g) sample GV07.

samples. The use of HSI, in the SWIR range (1000-2500 nm) gave a full topological assessment (i.e. mapping) of the different products present on painted mortar surfaces. HIS based mapping confirmed the results obtained by Raman spectroscopy and optical microscopy analysis. The use of chemometric based processing logics on the collected hyperspectral data was fundamental to identify the various pigment-binder mixtures present in the analysed samples. The proposed approach results particularly suitable to be applied, not only at laboratory scale, but also in situ, allowing to obtain the mapping of wide painted surfaces with their characteristics such as lacunae, alterations, typology of pigments and binders. etc.

Acknowledgments

The authors wish to thank Dr. Stefano Musco, Soprintendenza Speciale ai Beni Archeologici di Roma, Responsible of the Eastern Suburbs of Rome and the archeological site of Gabii and Dr. Cristina D'Agostini, Archaeologist at the same Soprintendenza, for their availability to allowing the analysis of Roman plaster samples. The authors wish to thank anonymous referees for their constructive comments.

References

Ballabio D. and Consonni V. (2013) - Classification tools in chemistry. Part 1: linear models. PLS-DA. *Analytical Methods*, 5, 3790-3798.

Bevilacqua N., Borgioli L. and Adrover Gracia I. (2010) - I pigmenti nell'arte dalla preistoria alla rivoluzione industriale. Casa Editrice Il Prato, Padova, Italy, 210-213.

Bro R. and Smilde A.K. (2014) - Principal component analysis. *Analytical Methods*, 6, 2812-2831.

Capobianco G., Bonifazi G., Prestileo F. and Serranti S. (2014) - Pigment identification in pictorial layers by HyperSpectral Imaging, Proc. SPIE 9106, Advanced Environmental, Chemical, and Biological Sensing Technologies XI, 91060B, 22 May 2014, doi:10.1117/12.2049941.

Capobianco G., Prestileo F., Serranti S. and Bonifazi G. (2014b) - Hyperspectral imaging for early detection of alteration phenomena in paint layers. Proceedings of VIII AIAr Conference, Bologna, 5-7 February 2014. http://www.associazioneaiar.com/cms/sites/default/files/Extended_abs_2014/CeD_poster/Capobianco%20et%20al.pdf.

Cucci C., Casini A., Picollo M. and Stefani L. (2013) - Extending hyperspectral imaging from Vis to NIR spectral regions: a novel scanner for the in-depth analysis of polychrome surfaces, Proc. SPIE 8790, Optics for Arts, Architecture, and Archaeology IV, 879009, 30 May 2013, doi:10.1117/12.2020286.

Gaffey S.J. (1986) - Spectral reflectance of-carbonate minerals in the visible and near infrared (0.35-2.55 microns): calcite, aragonite, and dolomite. *American Mineralogist*, 71, 151-162.

Geladi P., Grahn J. and Burger H. (2007) - Multivariate images, hyper-spectral imaging: background and equipment, in Grahnand H., Geladi P., Chichester W. (eds.), Techniques and Applications of Hyperspectral Image Analysis, 1-14.

Submitted, January 2015 - Accepted, May 2015